Results of the Department of Space Physics, Institute of Atmospheric Physics, Czech Academy of Sciences, published in 2016

1. Propagation of equatorial noise to low altitudes: Decoupling from the magnetosonic mode

Equatorial noise (often phenomenologically described as magnetosonic waves in the literature) is a natural electromagnetic emission, which is generated by instability of ion distributions and which can interact with electrons in the Van Allen radiation belts. We used multicomponent electromagnetic measurements of the DEMETER spacecraft to investigate if equatorial noise propagates inward down to the Earth. Analysis of a selected event recorded under disturbed geomagnetic conditions showed that equatorial noise can be observed at an altitude of 700 km, while propagating radially downward as a superposition of spectral lines from different distant sources observed at frequencies both below and above the local proton cyclotron frequency. Changes in the local ion composition encountered by the waves during their inward propagation disconnect the identified wave mode from the low-frequency magnetosonic mode. The local ion composition also induces a cutoff which prevents the waves from propagating down to the ground.

Reference:

Santolík, O., M. Parrot, and F. Němec (2016), Propagation of equatorial noise to low altitudes: Decoupling from the magnetosonic mode, Geophys. Res. Lett. 43, 6694-6704, doi:10.1002/2016GL069582.

Related references:

Parrot, M., F. Němec, **O. Santolík**, and N. Cornilleau-Wehrlin (2016), Equatorial noise emissions with a quasiperiodic modulation observed by DEMETER at harmonics of the O+ ion gyrofrequency, J. Geophys. Res. Space Physics, 121, 10,289-10,302, doi:10.1002/2016JA022989 Němec, F., M. Parrot, and O. Santolík (2016), Equatorial noise emissions observed by the DEMETER spacecraft during geomagnetic storms, J. Geophys. Res. Space Physics, 121, 9744-9757, doi:10.1002/2016JA023145

Sarno-Smith, L. K., M. W. Liemohn, R. M. Skoug, **O. Santolik**, et al. (2016), Hiss or equatorial noise? Ambiguities in analyzing suprathermal ion plasma wave resonance, J. Geophys. Res. Space Physics, 121, 9619–9631, doi:10.1002/2016JA022975

(Figure below) *Example of the burst-mode observations of the DEMETER spacecraft on 12 April 2005. Frequency-time plots of (a) the sum of the power-spectral densities of three orthogonal electric field components, (b) the sum of the power-spectral densities of three orthogonal magnetic field components, (c) the ellipticity of the magnetic field polarization with a sign corresponding to the sense of polarization, (d) the ellipticity of the electric field polarization with a sign corresponding to the sense of polarization, (e) the angle between the wave vector and the background magnetic field, (f) azimuth of the wave vector with respect to the outward direction, positive eastward, (g) the angle between the Poynting vector and the background magnetic field, and (h) azimuth of the Poynting vector with respect to the outward direction. A color scale is given on the right-hand side of each plot. . The local proton cyclotron frequency is given by a black solid line in each plot. Time is given in UT on the bottom, as well as the geomagnetic latitude of the spacecraft.*

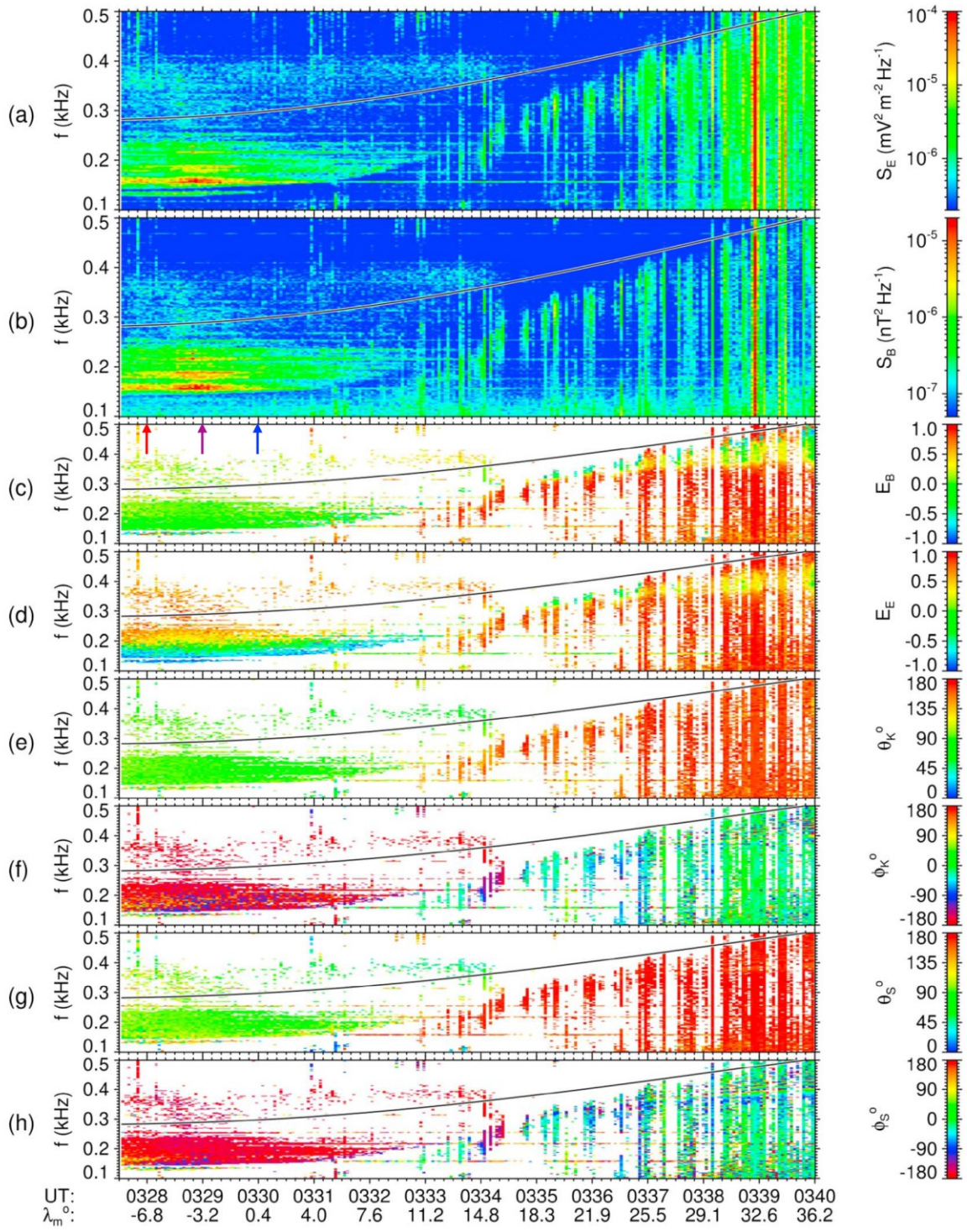
(a)
(b)
(c)
(d)
(e)
(f)
(g)
(h)
f (kHz)
0.5
0.4
0.3
0.2
0.1
S_E ($mV^2 m^{-2} Hz^{-1}$)
10^{-4}
10^{-5}
10^{-6}
S_B ($nT^2 Hz^{-1}$)
10^{-5}
10^{-6}
10^{-7}
E_B
E_E
1.0
0.5
0.0
-0.5
-1.0
θ_K^o
ϕ_K^o
θ_S^o
ϕ_S^o
180
135
90
45
0
-90
-180
UT:
λ_m^o:
0328 -6.8
0329 -3.2
0330 0.4
0331 4.0
0332 7.6
0333 11.2
0334 14.8
0335 18.3
0336 21.9
0337 25.5
0338 29.1
0339 32.6
0340 36.2

2. Poynting vector and wave vector directions of equatorial chorus

We presented new results on wave vectors and Poynting vectors of chorus rising and falling tones on the basis of 6 years of THEMIS (Time History of Events and Macroscale Interactions during Substorms) observations. The majority of wave vectors was closely aligned with the direction of the ambient magnetic field (B_0). Oblique wave vectors were confined to the magnetic meridional plane, pointing away from Earth. Poynting vectors were found to be almost parallel to B_0.

We showed, for the first time, that slightly oblique Poynting vectors were directed away from Earth for rising tones and toward Earth for falling tones. For the majority of lower band chorus elements, the mutual orientation between Poynting vectors and wave vectors was explained by whistler mode dispersion in a homogeneous collisionless cold plasma. Upper band chorus required inclusion of collisional processes or taking into account azimuthal anisotropies in the propagation medium. Upper band chorus required inclusion of collisional processes or taking into account azimuthal anisotropies in the propagation medium. The latitudinal extension of the equatorial source region was limited to ±6° around the B_0 minimum or approximately ±5000 km along magnetic field lines.

We found increasing Poynting flux and focusing of Poynting vectors on the B_0 direction with increasing latitude. Also, wave vectors became most often more field aligned. A smaller group of chorus generated with very oblique wave normals tended to stay close to the whistler mode resonance cone. This suggested that close to the equatorial source region (within ∼20° latitude), a wave guidance mechanism was relevant, for example, in ducts of depleted or enhanced plasma density.

Reference:

Taubenschuss, U., O. Santolik, H. Breuillard, W. Li, and O. Le Contel (2016), Poynting vector and wave vector directions of equatorial chorus, J. Geophys. Res. Space Physics, 121, doi:10.1002/2016JA023389.

Related references:

Santolík, O., Multi-dimensional Analysis of Whistler-mode Waves in the Radiation Belt Region, in Waves, Particles, and Storms in Geospace A Complex Interplay, Edited by Georgios Balasis, Ioannis A. Daglis, and Ian R. Mann, Oxford University Press, 2016, ISBN 9780198705246.

Li, W., **O. Santolik**, J. Bortnik, R. M. Thorne, C. A. Kletzing, W. S. Kurth, and G. B. Hospodarsky (2016), New chorus wave properties near the equator from Van Allen Probes wave observations, Geophys. Res. Lett., 43,4725-4735, doi:10.1002/2016GL068780.

Parrot, M., **O. Santolík**, and F. Nemec (2016), Chorus and chorus-like emissions seen by the ionospheric satellite DEMETER, J. Geophys. Res. Space Physics, 121, 3781-3792, doi:10.1002/ 2015JA022286.

Ripoll, J.-F., G. D. Reeves, G. S. Cunningham, V. Loridan, M. Denton, **O. Santolík**, W. S. Kurth, C. A. Kletzing, D. L. Turner, M. G. Henderson, and A. Y. Ukhorskiy (2016), Reproducing the observed energy-dependent structure of Earth's electron radiation belts during storm recovery with an event-specific diffusion model, Geophys. Res. Lett., 43, 5616-5625, doi:10.1002/2016GL068869.

Hospodarsky, G. B., W. S. Kurth, C. A. Kletzing, S. R. Bounds, **O. Santolík**, R. M. Thorne, W. Li, T. F. Averkamp, J. R. Wygant, and J. W. Bonnell (2016), Plasma Wave Measurements from the Van

Allen Probes, in Magnetosphere-Ionosphere Coupling in the Solar System, edited, pp. 127-143, John Wiley & Sons, Inc., doi:10.1002/9781119066880.ch10.

Hartley, D.P.,C.A.Kletzing, W. S. Kurth, S. R. Bounds, T. F. Averkamp, G. B. Hospodarsk y, J. R. Wygant, J. W. Bonnell, **O. Santolík**, and C. E. J. Watt (2016), Using the cold plasma dispersion relation and whistler mode waves to quantify the antenna sheath impedance of the Van Allen Probes EFW instrument, J. Geophys. Res. Space Physics, 121, 4590-4606, doi:10.1002/2016JA022501.

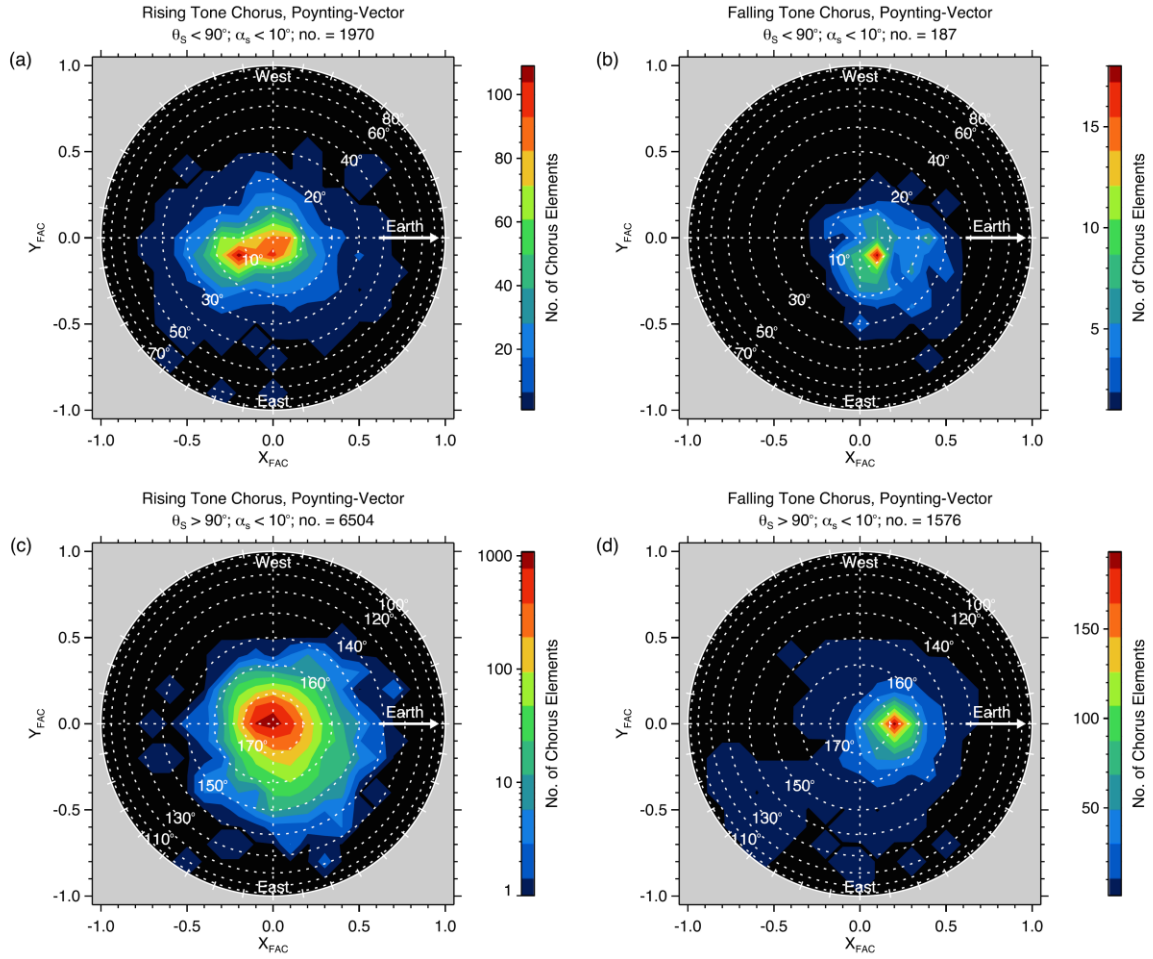

Poynting vector directions in the [x, y] plane of the FAC system. Panels are organized with regard to (a, c) rising tone chorus and (b, d) falling tone chorus and with regard to Poynting flux propagating (a, b) along the direction of B_0 or (c, d) against the direction of B_0. Count rates, i.e., the number of chorus elements per bin (0.1 × 0.1), are coded in rainbow colors.

3. Subionospheric propagation and peak currents of preliminary breakdown pulses before negative cloud-to-ground lightning discharges

We analyzed broadband electromagnetic measurements of pulse sequences occurring prior to first return strokes of negative cloud-to-ground lightning flashes. Signals generated by lightning discharges were recorded close to the thunderstorm by a magnetic field receiver and traveled up to 600km to three distant electric field receivers. We found that amplitudes of observed preliminary

breakdown pulses, as well as amplitudes of the corresponding return strokes, were attenuated approximately by 2 dB/100km when propagating in the Earth-ionosphere waveguide over mountainous terrain. Propagation simulations showed that there is a significant contribution of the sky wave signals in the waveforms observed beyond 500 km from their source. The estimated peak currents of the largest preliminary breakdown pulses reached over 60 kA. Such current pulses propagating through in-cloud lightning leader channels in a strong electric field may be able to initiate terrestrial gamma ray flashes.

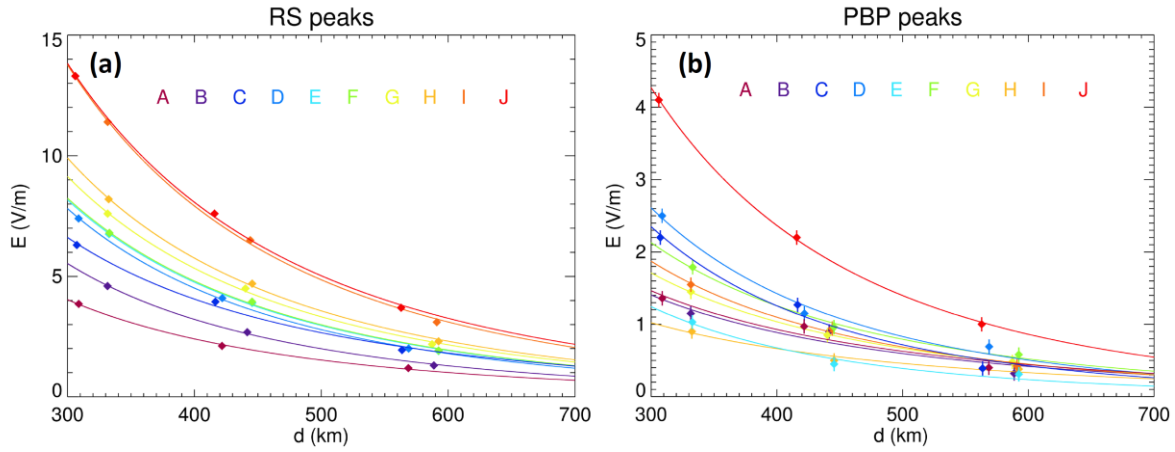

(a) Amplitudes of the RS pulses and (b) the corresponding dominant PBPs as a function of the distance from the source lightning stroke. Measured values (dots) and nonlinear least squares fits (lines) of the model are denoted by letters A–J and color coded from magenta to red according to the increasing RS peak current reported by MÉTÉORAGE for the 10 cases.

Reference:

Kolmašová, I., O. Santolík, T. Farges, S. A. Cummer, **R. Lán, and L. Uhlíř** (2016), Subionospheric propagation and peak currents of preliminary breakdown pulses before negative cloud-to-ground lightning discharges, Geophys. Res. Lett., 43, 1382-1391, doi:10.1002/ 2015GL067364.

4. Spatial distribution of Langmuir waves observed upstream of Saturn's bow shock by Cassini

We presented the spatial distribution and spectral properties of Langmuir waves observed upstream of Saturn's bow shock by the Cassini spacecraft. The entire 10 kHz wideband data set obtained between June 2004 and December 2014 was analyzed using an automated procedure. Almost 106 waveform snapshots with intense narrowband emissions in the frequency range of 1–10 kHz were detected. A typical wave spectrum exhibited a single intense peak (62% of all selected waveforms). However, spectra with a superposition of two (25%) or more (13%) intense peaks were also observed. Using magnetic field observations and a model of the bow shock, plasma wave activity across Saturn's foreshock was mapped. The plasma wave occurrence increased steeply behind the tangent magnetic field line, i.e, the sunward foreshock boundary, and rose with increasing distance from the tangential line into the downstream region. The single peak spectra were observed across the entire foreshock, while more complicated spectra were more likely measured deeper inside the foreshock and closer to the bow shock. We confirmed that the most intense waves occurred close to the tangent point and that their intensity decreased both deeper in the foreshock and along the tangential line.

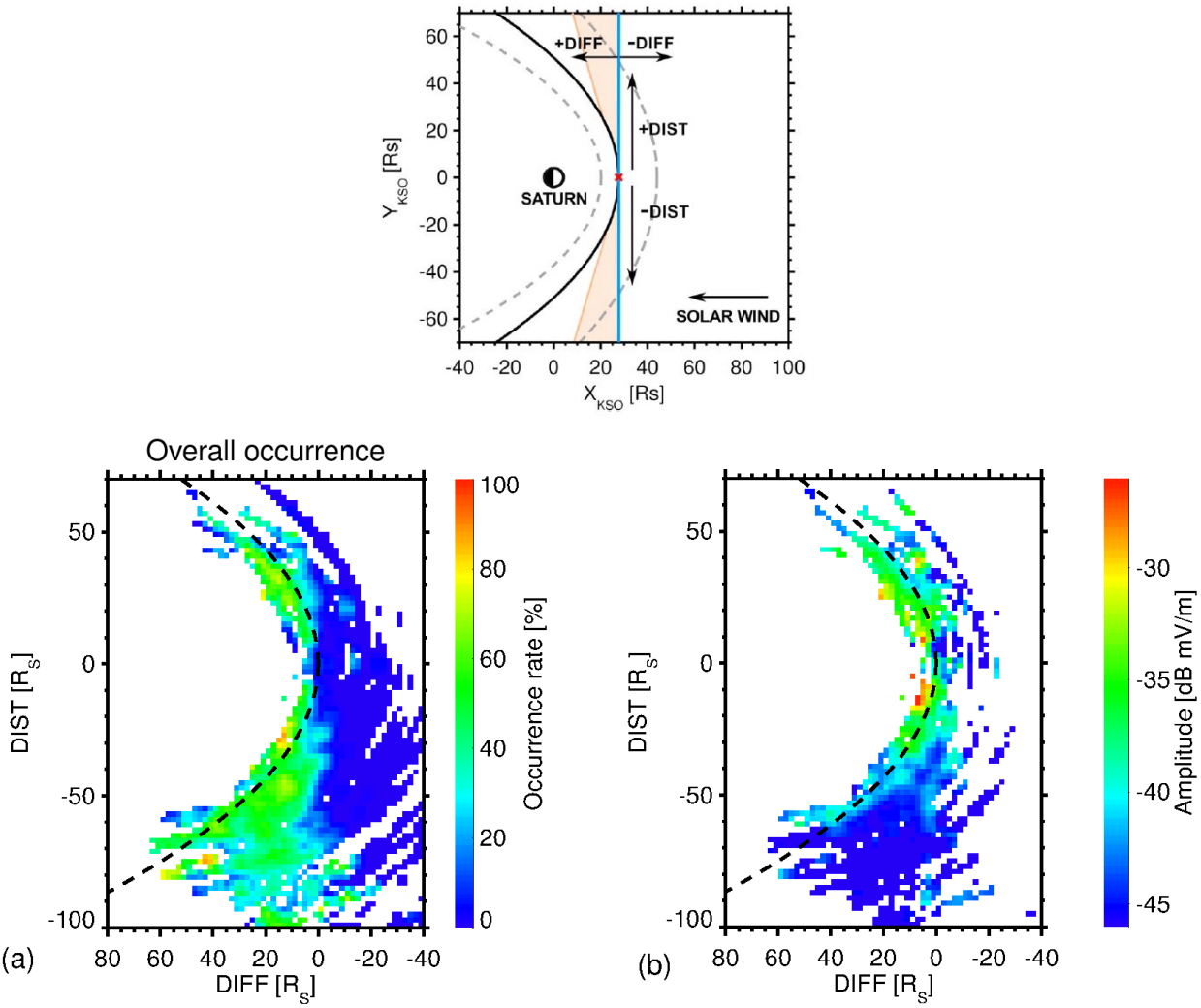

(top) Geometry of the Saturn's electron foreshock (orange color) in KSO coordinates for an 90° angle between the solar wind direction and interplanetary magnetic field (blue solid line). The gray dotted line indicates the lower and upper limit of the bow shock position obtained by the Went et al. [2011] model. The bow shock position used in the study is shown by the black solid line. The red cross defines the position of the tangent point. (bottom) Results of the Langmuir wave survey for 2004 through 2014. (a) Number of WBR waveforms captured beyond the bow shock as a function of foreshock position. (b) Overall occurrence rate of Langmuir waves observed outside Saturn's bow shock as a function of foreshock position.

Reference:

Píša, D., O. Santolík, G. B. Hospodarsky, W. S. Kurth, D. A. Gurnett, and **J. Souček** (2016), Spatial distribution of Langmuir waves observed upstream of Saturn's bow shock by Cassini, J. Geophys. Res. Space Physics, 121, 7771–7784, doi:10.1002/2016JA022912.

Related reference:

Menietti, J. D., P. H. Yoon, **D. Píša**, S.-Y. Ye, **O. Santolík**, C. S. Arridge, D. A. Gurnett, and A. J. Coates (2016), Source Region and Growth Analysis of Narrowband Z-mode Emission at Saturn, J. Geophys. Res. Space Physics, 121, doi:10.1002/2016JA022913.

5. Propagation properties of quasiperiodic VLF emissions observed by the DEMETER spacecraft

Quasiperiodic (QP) emissions are electromagnetic waves in the frequency range of about 0.5–4 kHz observed in the inner magnetosphere that exhibit a periodic time modulation of the wave intensity, with modulation periods from a few seconds up to 10 min. We presented results of a detailed wave analysis of nearly 200 events measured by the low-altitude Detection of Electro-Magnetic Emissions Transmitted from Earthquake Regions (DEMETER) spacecraft. Upper frequency range of studied emissions was limited to 1 kHz due to the sampling rate of the analyzed data. We found that QP emissions propagated nearly field aligned at larger geomagnetic latitudes; they became more oblique at midlatitudes and eventually perpendicular to the ambient magnetic field at the geomagnetic equator and thus perpendicular to the Earth's surface, allowing their downward propagation through the ionosphere. The observed propagation pattern was consistent with the source of missions located in the equatorial region at larger radial distances.

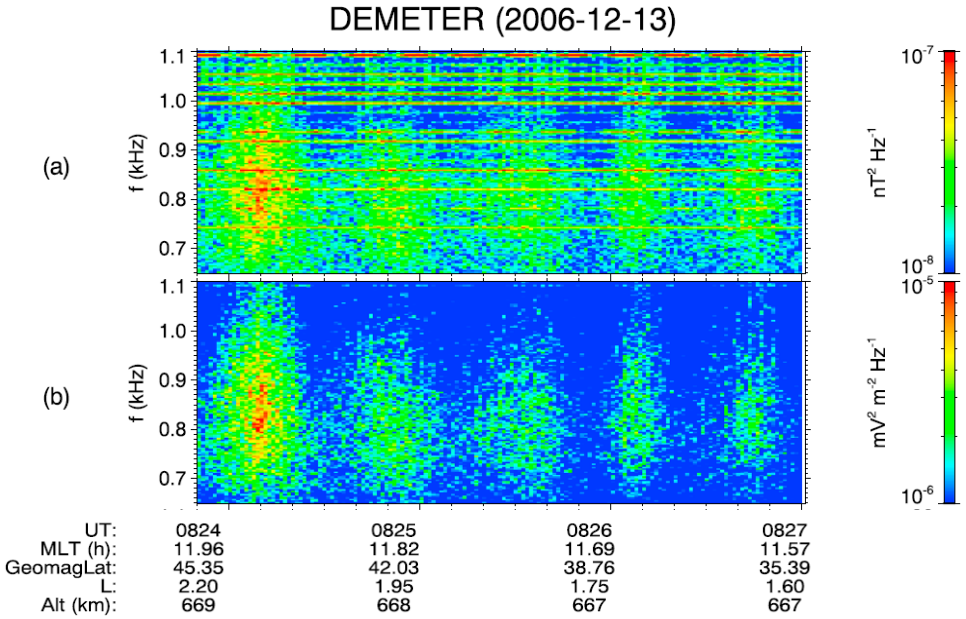

Frequency-time spectrogram of a QP event measured on 13 December 2006. (a, b) Power spectral density of magnetic and electric field fluctuations, respectively.

Reference:

Hayosh, M., F. Nemec, **O. Santolík**, and M. Parrot (2016), Propagation properties of quasiperiodic VLF emissions observed by the DEMETER spacecraft, Geophys. Res. Lett., 43, 1007-1014, doi:10.1002/2015GL067373.

Related references:

Nemec, F., G. Hospodarsky, J. S. Pickett, **O.Santolik**, W. S.Kurth, and C.Kletzing (2016), Conjugate observations of quasiperiodic emissions by the Cluster, Van Allen Probes, and THEMIS spacecraft, J. Geophys. Res. Space Physics, 121, 7647-7663, doi:10.1002/2016JA022774.

Martinez-Calderon, K., K. Shiokawa, Y. Miyoshi, K. Keika, M. Ozaki, I. Schofield, M. Connors, C.Kletzing, **M. Hanzelka, O. Santolik**, and W. S. Kurth. (2016), ELF/VLF wave propagation at subauroral latitudes: Conjugate observation between the ground and Van Allen Probes A, J. Geophys. Res. Space Physics, 121, doi:10.1002/2015JA022264.

6. Cluster observations of reflected EMIC-triggered emission

On 19 March 2001, the Cluster fleet recorded an electromagnetic rising tone on the nightside of the plasmasphere. The emission was found to propagate toward the Earth and toward the magnetic equator at a group velocity of about 200 km/s. The Poynting vector was mainly oblique to the background magnetic field and directed toward the Earth. The propagation angle became more oblique with increasing magnetic latitude. Each rising tone was more field aligned for higher frequencies. Comparing our results to previous ray tracing analysis we concluded that this emission was a triggered electromagnetic ion cyclotron (EMIC) wave generated at the nightside plasmapause. We detected the wave just after its reflection in the plasmasphere. The reflection made the tone slope shallower. This process can contribute to the formation of pearl pulsations.

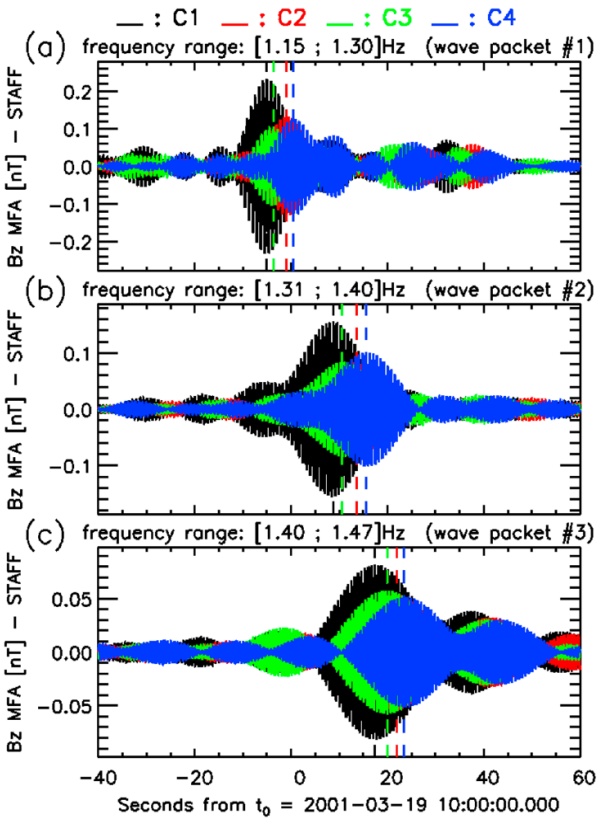

Field-aligned component of filtered magnetic waveforms observed by Cluster spacecraft around t0 for (a–c) three frequency ranges. Vertical dashed lines mark the waveform maximum recorded at each spacecraft during the displayed time and frequency ranges.

Reference:

Grison, B., F. Darrouzet, **O. Santolík**, N. Cornilleau-Wehrlin, and A. Masson (2016), Cluster observations of reflected EMIC-triggered emission, Geophys. Res. Lett., 43, 4164-4171, doi:10.1002/2016GL069096.

Related reference:

Sigsbee, K., C. A. Kletzing, C. W. Smith, R. MacDowall, H. Spence, G. Reeves, J. B. Blake, D. N. Baker, J. C. Green, H. J. Singer, C. Carr, and **O. Santolík** (2016), Van Allen Probes, THEMIS, GOES, and Cluster observations of EMIC waves, ULF pulsations, and an electron flux dropout, J. Geophys. Res. Space Physics, 121, 1990-2008, doi:10.1002/2014JA020877.

7. Interplanetary solar radio emissions associated with a coronal mass injection

Coronal mass ejections (CMEs) are large-scale eruptions of magnetized plasma that may cause severe geomagnetic storms if Earth directed. We reported a rare instance with comprehensive in situ and remote sensing observations of a CME combining white-light, radio, and plasma measurements from four different vantage points. For the first time, we successfully applied a radio direction-finding technique to an interplanetary type II burst detected by two identical widely separated radio receivers. The derived locations of the type II and type III bursts were in general agreement with the white-light CME reconstruction. We found that the radio emission arose from the flanks of the CME and that it was most likely associated with the CME-driven shock. Our work demonstrated the complementarity between radio triangulation and 3D reconstruction techniques for space weather applications.

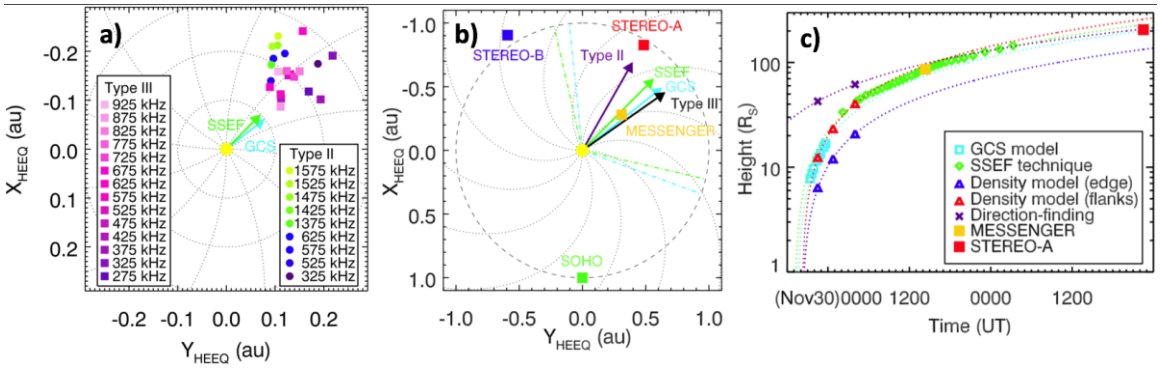

(a) Propagation analysis of radio measurements. Radio source locations of type II (circles) and type III (squares) bursts for four time-frequency intervals in the XY_{HEEQ} plane. Colors denote frequencies. The cyan and green arrows indicate the CME propagation directions obtained by the GCS model and the SSEF technique, respectively. The Sun is at (0, 0). (b) Positions of the spacecraft in the solar equatorial plane on 2013 November 29. The purple and arrows indicate average directions of type II and type III bursts, respectively. The cyan and green arrows indicate the CME propagation directions obtained by the GCS model and the SSEF technique, respectively. Dotted–dashed lines show the CME half-width. (c) Kinematics of the CME and radio sources between 2013 November 29 and December 1. Dotted lines are linear fits.

Reference:

Krupař, V., J. P. Eastwood, **O. Krupařová, O. Santolík, J. Souček**, J. Magdalenic, A. Vourlidas, M. Maksimovic, X. Bonnin, V. Bothmer, N. Mrotzek, A. Pluta, D. Barnes, J. A. Davies, J. C. Martínez Oliveros, and S. D. Bale (2016), An analysis of interplanetary soalr radio emissions associated with a coronal mass injection, The Astrophysical Journal Letters, 823:L5 (7pp), doi: 10.3847/2041-8205/823/1/L5.

Related reference:

Mäkelä, P., Gopalswamy, N., Reiner, M. J., Akiyama, S., and **Krupař, V.** (2016), Source regions of the type II radio burst observed during a CME–CME interaction on 2013 May 22, Astrophysical Journal, 827, 2, pp. 141/1-141/7.

Department of Space Physics, Institute of Atmospheric Physics of the Czech Academy of Sciences in 2016

1. Marek Basovník, PhD student, 60% FTE
2. Benjamin Grison, research scientist
3. Michajlo Hajoš, research scientist
4. Miroslav Hanzelka, MSc student, 20% FTE, since May 1
5. Miroslav Horký, postdoctoral associate
6. Zuzana Sochorová (née Hrbáčková), PhD student, 70% FTE, until May 30
7. Petr Kašpar, postdoctoral associate
8. Vratislav Krupař, research scientist, 20% FTE until October 31, 100% FTE since November 1
9. Oksana Krupařová, research scientist
10. Eva Macúšová, postdoctoral associate, until August 31
11. Radek Lán, research engineer
12. Martin Pauer, research engineer, 20% FTE, since August 15
13. David Píša, postdoctoral associate
14. Martin Popek, TLE observer, 25% FTE, since August 1
15. Ondřej Santolík, senior research scientist, head of the department
16. Jan Souček, senior research scientist, deputy head of the department
17. Ulrich Taubenschuss, research scientist
18. Alexander Tomori, PhD student, 50% FTE
19. Hana Zemanová, PhD student, 50% FTE